

Probing color reconnection with underlying-event observables at the LHC energies

Antonio Ortiz

*Instituto de Ciencias Nucleares, Universidad Nacional Autónoma de México,
Ciudad de México, Del. Coyoacán 04510, México*

Lizardo Valencia Palomo

*Departamento de Investigación en Física, Universidad de Sonora,
Blvd Luis Encinas y Rosales S/N, Col. Centro, Hermosillo, Sonora, México*

Abstract

In this work we study the underlying-event (UE) activity as a function of the highest jet or charged-particle transverse momentum (p_T^{jet} or p_T^{leading}) in terms of number and summed- p_T densities of charged particles in the azimuthal region transverse to the leading jet or particle direction. Contrary to inelastic pp LHC data, the UE observables normalised to the charged-particle density obey an approximate Koba-Nielsen-Olesen (KNO) scaling. Based on PYTHIA 8.2 simulations of pp collisions at LHC energies, we show that the small breaking of the KNO scaling is due to the increasing importance of multiple partonic interactions (MPI) at higher \sqrt{s} . This in turn makes that with increasing energy, the p_T spectra in the UE get harder than in inelastic pp collisions.

Color reconnection (CR) models the interactions among outgoing partons just before the hadronization, therefore it modifies the p_T -spectral shape. Motivated by this, we studied the UE activity considering charged particles within different p_T intervals in pp collisions at $\sqrt{s} = 7$ TeV. Although MPI saturation for $p_T^{\text{jet}} > 10$ GeV/ c , the UE still increases with increasing p_T^{jet} . We demonstrate that the saturation of both number and summed- p_T densities,

*Corresponding author

Email address: `lizardo.valencia@unison.mx` (Lizardo Valencia Palomo)

which are commonly claimed, are only observed for low- p_T charged particles ($0.5 < p_T < 2 \text{ GeV}/c$). Moreover, for the p_T -integrated case ($p_T > 0.5 \text{ GeV}/c$) the summed- p_T density is not sensitive to the variation of CR, however at low- p_T it is reduced with increasing CR, whereas an opposite behavior is found at intermediate- p_T ($2 < p_T < 10 \text{ GeV}/c$). Finally, we show that CR produces flow-like behavior only in the UE region and the effects are reduced with increasing p_T^{jet} due to the hardening of UE. The outcomes encourage the measurement of inclusive and identified charged-particle p_T spectra (over a wide range of p_T) associated to UE aimed at better understanding the similarities between pp and heavy-ion data discovered at the LHC.

Keywords: Hadron-Hadron scattering, Underlying Event, LHC

1. Introduction

In the context of event generators, one single inelastic (non-diffractive) proton-proton (pp) collision can be split into two components: the main hard partonic scattering and the underlying event (UE). The latter includes initial- and final-state radiation (ISR/FSR), multiple partonic interactions (MPI) and the fragmentation of beam remnants resulting from the hadronization of the partonic constituents that did not participate in any scatter. On top of that, color reconnection (CR) is a microscopic mechanism that describes the interactions that can occur between color fields during the hadronization transition. It is a key ingredient which is needed to explain the increase of the average transverse momentum as a function of charged-particle multiplicity [1] and the multiplicity-dependent event shape studies [2]. The importance of the UE relies on the fact that it can shed light in the search for new physics phenomena at hadron colliders [3] or even in the quest for precise Standard Model measurements [4].

The UE observables have been measured in $p\bar{p}$ collisions in dijet and Drell-Yan processes at CDF at $\sqrt{s} = 1.8$ and 1.96 TeV [5, 6]. At the start of the LHC most of the existing Monte Carlo models were tuned using Tevatron data. In this sense, early measurements provided by the ATLAS experiment [7] showed

clear differences between event generators and data. Latest results have shown an improvement on the description of the UE by the new Monte Carlo tunes [8].
21 However, we should keep in mind that the modelling of UE is more challenging than traditionally assumed because recent results suggest the unexpected presence of heavy ion-like behavior in pp data [9, 10, 11, 12]. We should therefore
24 go beyond the traditional UE analysis for better understanding the similarities between pp and heavy-ion data.

In order to understand the physics behind high-multiplicity pp collisions, we have performed several studies using PYTHIA 8 [13] event generator. We have found that CR together with MPI can produce radial flow patterns via boosted color strings [14]. The analysis as a function of event multiplicity allows to study events with different amount of MPI, however we have shown
30 that high-multiplicity pp collisions are effected by the so-called fragmentation bias [15, 16]. Moreover, for a fixed amount of MPI CR strongly modifies the charged-particle multiplicity, therefore a selection based on multiplicity does not
33 permit the isolation of CR effects in events with the same MPI activity. In this work we propose to exploit the usage of UE in order to increase the sensitivity
36 to events with multiple semi-hard scatterings instead to biased fragmentation of high transverse momentum jets. Similar ideas have been proposed in order to disentangle auto-correlation effects from other physical phenomena by
39 measuring the charged-particle multiplicity in the UE region [17].

Given that heavy-ion data feature remarkable differences between the particle production associated to bulk (everything outside the jet peaks) and jets [18, 42 19], we have decided to perform an analogous analysis in pp collisions simulated with PYTHIA 8. The advantage is that cutting on the highest charged-particle transverse momentum (p_T^{leading}) or highest jet p_T (p_T^{jet}) it is possible to select
45 events with larger (and nearly constant) MPI activity than that associated to inelastic events. This allows to enhance color-reconnection effects on the hadronization.

48 Specifically, in this paper we study the modification of the traditional UE observables when charged particles within different p_T intervals are considered.

We also aim to understand how the underlying-event activity is affected when
 51 either p_T^{jet} or \sqrt{s} are varied. The analysis is not restricted to the traditional
 average quantities, instead we study the p_T spectra of unidentified and identified
 charged particles within UE environments modified with a selection on p_T^{jet} . The
 54 measurements of the p_T spectra sensitive to UE as a function of p_T^{jet} are proposed
 as a tool to probe the QCD Monte Carlo picture using LHC data.

The article is organised as follows: section 2 provides information about the
 57 event and particle selection for the simulations, section 3 discusses the energy
 dependence of the UE in terms of the number and summed- p_T densities, sec-
 tion 4 presents the results on how CR affects the UE observables and the p_T
 60 distribution of identified charged particles, and finally section 5 contains the
 summary and outlook.

2. Simulations and analysis

63 Quantities sensitive to the UE are constructed as follows. The perpendic-
 ular plane to the beam axis is segmented into three regions depending on the
 azimuthal angular difference ($\Delta\phi$) relative to the leading object (e.g. jet or
 66 charged particle) axis. Unless specified, those particles with $\pi/3 < |\Delta\phi| < 2\pi/3$
 (transverse side) are the only ones used for the present analysis since they are
 the most sensitive to UE. The underlying-event observables are defined as the
 69 mean number of charged particles per pseudorapidity unit and per azimuthal
 separation unit ($\langle N_{\text{ch}}/\Delta\eta\Delta\phi \rangle$) and the mean scalar sum of transverse momen-
 tum per pseudorapidity unit and per azimuthal separation unit ($\langle \Sigma p_T/\Delta\eta\Delta\phi \rangle$).
 72 hereafter $\langle N_{\text{ch}}/\Delta\eta\Delta\phi \rangle$ and $\langle \Sigma p_T/\Delta\eta\Delta\phi \rangle$ are referred to as number density and
 summed- p_T density, respectively. PYTHIA 8.212 [13] tune Monash 2013 [20],
 hereafter referred to as PYTHIA 8, was used to simulate inelastic pp collisions at
 75 the LHC energies. Since simulations are intended to be compared to CMS [21],
 ATLAS [8] and ALICE [22] results available on HEPData [23], different selec-
 tions at particle and event levels were implemented:

- 78 1. The comparison of simulations with CMS data (pp collisions at $\sqrt{s} = 0.9$

and 7 TeV) requires a leading jet with transverse momentum larger than 1 GeV/ c within the pseudorapidity interval: $|\eta| < 2$. Jets are defined using the SISCone algorithm [24] as implemented in FastJet 3.3 [25] with the clustering radius given as $R = \sqrt{(\Delta\phi)^2 + (\Delta\eta)^2} = 0.5$. Furthermore, jets are built using charged particles with $p_T > 0.5$ GeV/ c and $|\eta| < 2.5$. The UE observables are computed using charged particles within $|\eta| < 2$ and $p_T > 0.5$ GeV/ c . Notice the η range of particles used to build the jets is larger than that of particles in the UE in order to avoid a kinematic bias.

2. The comparison with ALICE data (pp collisions at $\sqrt{s} = 0.9$ and 7 TeV) requires charged particles with $p_T > 0.5$ GeV/ c and $|\eta| < 0.8$ with the transverse momentum of the leading charged particle above 0.5 GeV/ c .
3. The comparison with ATLAS data (pp collisions at $\sqrt{s} = 13$ TeV) requires charged particles with $p_T > 0.5$ GeV/ c and $|\eta| < 2.5$ with the transverse momentum of the leading charged particle above 1 GeV/ c .

In all cases the configuration used in PYTHIA 8 was the following: Beams:idA = 2212, Beams:idB = 2212, Beams:eCM = 900 (7000 and 13000), Tune:pp = 14 and SoftQCD:inelastic = on.

3. Energy dependence of the underlying event

In a previous publication [26], we have shown that within 10% the UE observables as a function of p_T^{leading} collapse on \sqrt{s} -independent curves once they are scaled to the corresponding average charged-particle density ($dN_{\text{ch}}/d\eta^{\text{inelastic}}$). This quantity is obtained for inelastic pp collisions at a given center-of-mass energy. In this paper we want to trace back the origin of the small imperfection of the scaling behavior, i.e. its validity within 10%. Instead of using ATLAS UE data (measured as a function of p_T^{leading}), now we use the CMS data since they are reported for a wide p_T^{jet} interval. This allows the study of pp events with exceptional high- p_T jets. In order to obtain the charged-particle density, the transverse momentum distributions of charged particles in pp collisions at $\sqrt{s} = 0.9$ and 7 TeV [27, 28] were integrated for $|\eta| < 2.4$ and $p_T > 0.5$ GeV/ c .

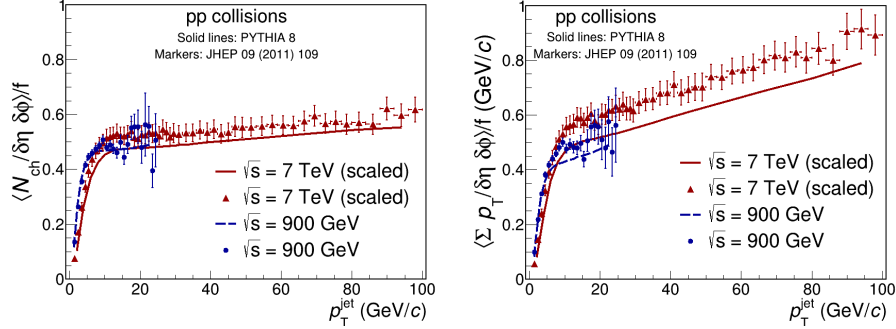


Figure 1: (Color online). The number density (left) and the summed- p_T density (right) as a function of p_T^{jet} in the UE region. A factor f that takes into account the relative charged-particle density increase from 0.9 to 7 TeV has been applied. Data are shown as markers and the error bars represent the total uncertainties (the one measured by CMS and the associated to f). Solid lines are the results obtained with PYTHIA 8.

108 The total uncertainties (quadratic sum of statistical and systematic uncertain-
 ties) associated to the p_T spectrum were propagated to the integral and assigned
 as systematic uncertainty to $\langle dN_{\text{ch}}/d\eta \rangle^{\text{inelastic}}$. For pp collisions at $\sqrt{s} = 0.9$ and
 111 7 TeV, the computed values were $\langle dN_{\text{ch}}/d\eta \rangle^{\text{inelastic}} = 1.20 \pm 0.04$ and 2.33 ± 0.11 ,
 respectively. Therefore, the relative variation (f) of the average charged-particle
 density in pp collisions at $\sqrt{s} = 7$ TeV with respect to pp collisions at $\sqrt{s} = 0.9$
 114 TeV was found to be $f = 1.94 \pm 0.11$.

Figure 1 shows the number (left panel) and the summed- p_T (right panel)
 densities as a function of p_T^{jet} after scaling by a $1/f$ factor. Little or no energy
 117 dependence is observed after the implementation of the scaling factor. This is
 what we called “universality of UE” in our previous work where p_T^{leading} was
 used instead [26]. The results are compared with PYTHIA 8 simulations since
 120 it reproduces very well many features of LHC data. We observe that the scaling
 properties hold up to $p_T^{\text{jet}} = 25$ GeV/ c . Regarding the behavior of data, a steep
 rise of the underlying activity with increasing p_T^{jet} is observed. This fast rise
 123 is followed by a change of the slope above $p_T^{\text{jet}} \sim 10$ GeV/ c . The change of
 the slope is understood as due to very small impact parameter pp collisions

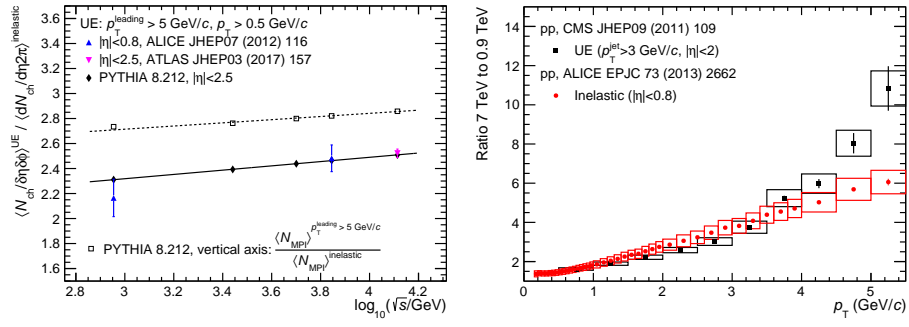


Figure 2: (Color online). Left: Energy dependence of the number density (UE) normalised to the average charged-particle density in inelastic events. PYTHIA 8 simulations of pp collisions at $\sqrt{s} = 0.9, 2.76, 5.02, 7$ and 13 TeV (full black markers) are compared to ALICE (full blue markers) and ATLAS data (full magenta markers). Similar ratios (empty markers) were obtained using the number of multiple partonic interactions (N_{MPI}). Right: UE transverse momentum distribution (associated to $p_T^{\text{jet}} > 3$ GeV/c) in pp collisions at 7 TeV normalized to the corresponding one at 0.9 TeV (black squares). Results are compared to analogous ratios for inelastic pp collisions at the same energies (red circles). Statistical and systematic uncertainties are represented as error bars and boxes around the data points, respectively. Data were obtained from [21, 29].

which yields to a saturation of the MPI activity. Different publications state
 126 that above $10 \text{ GeV}/c$ the UE observables saturate, reaching nearly constant
 values [22, 8, 30]. However, we want to stress the fact that both data and
 PYTHIA 8 still show a rise of the UE activity with increasing p_T^{jet} . In the next
 129 sections we discuss how color reconnection contributes to that behavior.

The universality of UE can be interpreted as the approximate Koba-Nielsen-
 Olesen (KNO) [31] scaling of the particle production associated to the UE. For
 132 this reason we studied the energy dependence of the KNO variable: number den-
 sity in the transverse side normalised to the charged-particle density (inelastic
 pp collisions). This ratio has been studied by ALICE using pp data at $\sqrt{s} = 0.9$
 135 and 7 TeV [22]. To obtain the numerator, ALICE fitted a first degree polynomial
 to the number density as a function of p_T^{leading} for $p_T^{\text{leading}} > 5 \text{ GeV}/c$. Within
 uncertainties the fit slope was found to be consistent with zero and the constant
 138 parameter was identified as the average number density in the transverse side.
 Potential correlations of the systematic uncertainties in different p_T bins were
 neglected. The left-hand side of Fig. 2 shows a comparison of the KNO variable
 141 as a function of $\log(\sqrt{s})$ measured by ALICE and ATLAS. ALICE data points
 were taken from [22] while the ATLAS point was derived following the strategy
 already described. PYTHIA 8 inelastic pp events were simulated in order to test
 144 the scaling of UE over the wide \sqrt{s} interval covered at the LHC. Going from pp
 collisions at $\sqrt{s} = 0.9$ to 13 TeV , PYTHIA 8 simulations show a $\sim 8\%$ increase
 of the KNO variable. Within uncertainties, the data exhibit the same trend.
 147 The small \sqrt{s} dependence is also observed if we consider the average number
 of MPI in events with $p_T^{\text{leading}} > 5 \text{ GeV}/c$ (central pp collisions) normalised to
 this same observable but in inelastic pp collisions (i.e. without any selection
 150 on p_T^{leading}). The ratio as a function of $\log(\sqrt{s})$ is described by a first degree
 polynomial with a slope parameter of 0.13, which is close to what is obtained
 using the number density (slope 0.17), suggesting a common origin.

153 In order to investigate the features of particle production associated to UE,
 in particular the excess of particles in UE with respect to inelastic pp collisions,
 we studied the p_T spectra of unidentified charged particles. The CMS collabo-

156 ration has reported such spectra for pp collisions at $\sqrt{s} = 0.9$ and 7 TeV. The
 UE corresponds to events with $p_T^{\text{jet}} > 3 \text{ GeV}/c$ within $|\eta| < 2$. To study the
 evolution of the p_T -differential particle production with increasing energy, the
 159 7 TeV p_T spectrum was normalized to the corresponding one at 0.9 TeV. The
 results are presented in the right-hand side of Fig. 2. An analogous ratio as
 a function of p_T was obtained using the p_T spectra of inelastic pp collisions
 162 at the same energies [29]. Within uncertainties, both ratios are consistent up
 to $p_T = 4 \text{ GeV}/c$. For higher p_T the ratio increases faster for the UE activity
 than for inelastic pp collisions. The results suggest that, with increasing \sqrt{s} ,
 165 intermediate- p_T particle production increases faster in the UE than in inelastic
 pp collisions. This effect could explain the faster rise of the number density in
 the UE relative to the corresponding inelastic events [22]. Transverse momen-
 168 tum distributions sensitive to UE for other \sqrt{s} and p_T^{jet} are needed in order to
 confirm the validity of this conclusion.

4. CR studies using UE observables

171 We have shown that, with increasing \sqrt{s} , the p_T spectra sensitive to UE get
 harder than that in inelastic events as a consequence of the \sqrt{s} dependence of
 MPI. Since in events with large number of MPI color reconnection modifies the
 174 particle production [14], CR effects on UE are expected. In order to quantify
 such effects we used the default CR model of PYTHIA 8 (MPI-based) . The
 model includes the reconnection probability (rr) to join low and high p_T par-
 177 tons. Therefore, rr (ColourReconnection:range in PYTHIA 8) allows to control
 the amount of interactions which partons feel just before the hadronization. For
 our study, we computed $\langle N_{\text{ch}}/\Delta\eta\Delta\phi \rangle$ and $\langle \Sigma p_T/\Delta\eta\Delta\phi \rangle$ in three different p_T
 180 ranges depending on the transverse momentum of the charged particles present
 in the UE: integrated ($p_T > 0.5 \text{ GeV}/c$), low ($0.5 < p_T < 2 \text{ GeV}/c$) and inter-
 mediate ($2 < p_T < 10 \text{ GeV}/c$) transverse momentum. Each p_T -dependent UE
 183 quantity was in turn computed for three different values of rr : 0, 1.8 and 10,
 corresponding to the minimum, nominal (tuned to LHC data [20]) and maxi-

mum possible values in PYTHIA 8. Moreover, the results presented here are
 186 obtained using leading jets within the CMS kinematic ranges, allowing the com-
 parison between data and PYTHIA 8 over a broad p_T^{jet} interval. Since we claim
 an approximate scaling of the particle production associated to UE, we report
 189 results only for pp collisions at $\sqrt{s} = 7$ TeV. The conclusions should hold for
 other energies.

Modification of the particle production at low and intermediate p_T . Figure 3
 192 shows the number density as a function of p_T^{jet} for pp collisions at $\sqrt{s} = 7$ TeV.
 For the p_T -integrated case, CMS data are compared with PYTHIA 8 simula-
 tions considering three different values of rr . Within uncertainties, data are
 195 well described by simulations with $rr \geq 1.8$. As expected, the number density
 decreases with increasing rr due to the reduction of the number of color strings
 that connect the outgoing partons. Though, the p_T^{jet} dependence of the number
 198 density is the same for the different rr values. For the low- p_T case, we observe
 the same rr ordering reported for the p_T -integrated case. However, the number
 density is reduced by $\sim 20\%$ relative to the p_T -integrated case. The number
 201 density associated to intermediate- p_T particles exhibits an opposite trend with
 increasing rr , i.e. going from low- to high- rr values the number density increases
 suggesting a hardening of UE with increasing rr .

204 The corresponding plots for the summed- p_T density are shown in Fig. 4.
 Contrary to the number density, this observable presents a steeper rise with
 increasing p_T^{jet} and no color-reconnection effects are visible for the p_T -integrated
 207 case. However, this does not happen when the summed- p_T density is calculated
 considering low- or intermediated- p_T charged particles. Namely, for low- p_T
 particles the summed- p_T density shows a saturation for $p_T^{\text{jet}} > 10$ GeV/ c . More-
 210 over, the summed- p_T density decreases with increasing values of rr (the CR
 effect amounts to 5%). For the intermediate- p_T case, the summed- p_T density
 rises with increasing p_T^{jet} more or less at the same rate that the p_T -integrated
 213 case.

In order to avoid any possible jet effect (at small values of $|\Delta\eta|$) that could

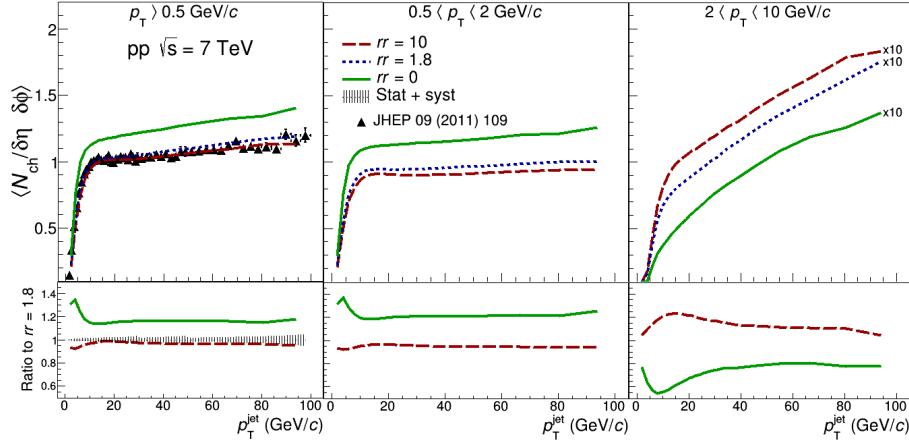


Figure 3: (Color online). The number density as a function of the p_T^{jet} for three different values of reconnection range. Results for the p_T -integrated case are displayed for both the CMS data and PYTHIA 8 simulations (left). Analogous results are shown for low- (middle) and intermediate- (right) p_T particles. Bottom panels show the variation of the number density with respect to $rr = 1.8$. Shaded areas around unity indicate the statistical and systematic uncertainty (added in quadrature) on CMS data.

bias the previous results, an extra cut on $|\Delta\eta|$ was tested. In this sense only
 216 particles with $|\Delta\eta| > 1.6$ were selected, but no significant differences were observed.

In short, the behavior of the number density as a function of p_T^{jet} is deter-
 219 mined by low-momenta particles while for summed- p_T density is determined by intermediate- p_T particles. It was verified that, qualitatively, the same behavior is obtained for both UE observables at $\sqrt{s} = 900 \text{ GeV}$. It is worth mentioning
 222 that UE measurements considering different p_T intervals are not available. Our work suggests the necessity of such measurements in order to test the picture of PYTHIA 8, i.e. the hardening of the UE structure with increasing p_T^{jet} (or \sqrt{s})
 225 by means of MPI and CR.

Flow-like effects within a hard UE environment. It has been shown that CR
 produces flow-like effects that increase with increasing $\langle N_{\text{MPI}} \rangle$ [14]. This is
 228 because the number of strings connecting scattered partons naturally increases

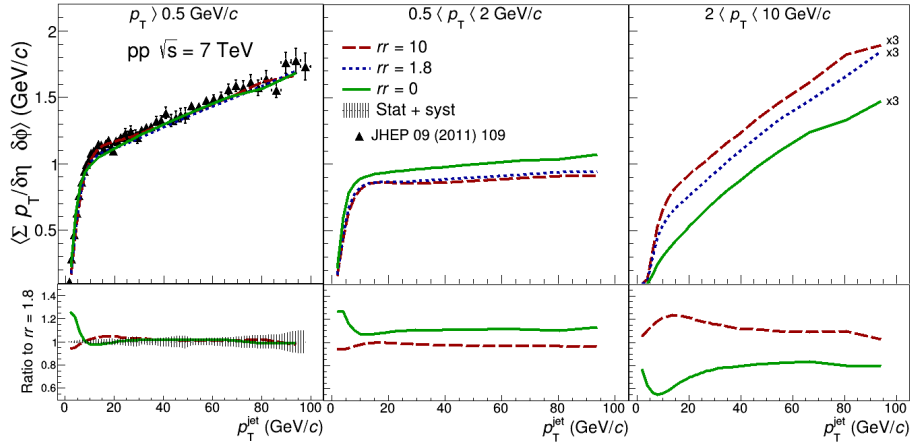


Figure 4: (Color online). The summed- p_T density as a function of the p_T^{jet} for three different values of reconnection range. Results for the p_T -integrated case are displayed for both the CMS data and PYTHIA 8 simulations (left). Analogous results are shown for low- (middle) and intermediate- (right) p_T particles. Bottom panels show the variation of the summed- p_T density with respect to $rr = 1.8$. Shaded areas around unity indicate the statistical and systematic uncertainty (added in quadrature) on CMS data.

with increasing $\langle N_{\text{MPI}} \rangle$. CR allows the color fields of the event to be redirected, relative to the case of color-separated MPI, in such a way that the total string
231 length is reduced. This produces a transverse boost to reconnected string pieces, that e.g. provides to heavier hadrons higher $\langle p_{\text{T}} \rangle$ [32]. It has been shown that in events with enhanced UE activity, relative to inelastic pp collisions, the
234 flow-like effects increase. This has been achieved by selecting highly-spherical events where no jet structure is present [33]. Motivated by the similarity of the event-shape selection results with those for heavy-ion collisions where the
237 proton-to-pion ratio (sensitive to radial flow [34]) is studied for the regions sensitive to bulk production and jet fragmentation, separately. We decided to perform an analogous Monte Carlo analysis but considering the underlying event
240 accompanying a very high- p_{T} jet. The goal of the study is to understand how the $p_{\text{T}}^{\text{jet}}$ selection affects observables sensitive to radial flow in the UE region.

Figure 5 shows the proton-to-pion ratio as a function of the hadron transverse
243 momentum in the underlying-event region for two $p_{\text{T}}^{\text{jet}}$ bins and for three different values of rr : 0, 1.8 and 10. The left-hand side of Figure 5 shows the results for $30 < p_{\text{T}}^{\text{jet}} < 40 \text{ GeV}/c$. Going from independent fragmentation ($rr = 0$) to the
246 largest value of rr , the proton yield is suppressed with respect to the pion one for $p_{\text{T}} < 2 \text{ GeV}/c$, whereas for intermediate transverse momentum the proton yield is enhanced relative to the pions. This is the mass effect attributed to
249 color reconnection that was previously reported for the inclusive event [14], i.e. without any separation of the soft and hard components. It is worth noting that the size of the bump shown in Fig. 5 is smaller than that seen in the
252 inclusive case [14]. The reduction is understood in terms of the hardness of the underlying event that increases with increasing $p_{\text{T}}^{\text{jet}}$. The right-hand side of Fig. 5 shows the results when we move from $30 < p_{\text{T}}^{\text{jet}} < 40 \text{ GeV}/c$ to higher jet
255 transverse momentum ($40 < p_{\text{T}}^{\text{jet}} < 100 \text{ GeV}/c$). Going from low- to high- $p_{\text{T}}^{\text{jet}}$ values the structure at $p_{\text{T}} = 3 \text{ GeV}/c$ is reduced. Moreover, the results show a smaller dependence on rr indicating that the ratio is more sensitive to the
258 fragmentation of hard partons.

Finally, in order to show the distinct behavior of the UE with respect to

jet fragmentation, Figure 6 presents the proton-to-pion ratio as a function of
 261 p_T obtained for the towards region ($|\Delta\phi| < \pi/3$). In particular, only pions
 and protons within $R < 0.5$ are considered. Notice that, opposite to Figures 3
 and 4, the ratios in the bottom panels of Figures 5 and 6 are performed relative
 264 to $rr = 0$. The reason is because in the latter case the goal is to quantify the
 flow-like effect, if any, that is observed when color reconnection is present.

Overall in Figure 6, the ratio is significantly smaller than the corresponding
 267 for the underlying-event region. For example, while for the transverse region
 the ratio shows a maximum amounting to ~ 0.22 at $p_T = 3 \text{ GeV}/c$; for the
 jet peak ($30 < p_T^{\text{jet}} < 40 \text{ GeV}/c$) it reaches 0.1 and the value is subsequently
 270 reduced with increasing p_T^{jet} . It is worth mentioning that although a color-
 reconnection effect is observed in the jet region as a consequence of the UE
 contamination, its effect is smaller than what is seen in the transverse side. The
 273 effects observed for the UE and jet regions are qualitatively similar to those
 measured in heavy-ion collisions resulting from the jet-bulk separation using
 leading-hadron correlations. The statement there [18] is that the flow-like peak
 276 observed in proton-to-pion ratio for the most central Pb-Pb collisions at the
 LHC energies is a medium effect.

The effects reported in this paper should be searched in data; the outcome
 279 would contribute to the understanding of the unexpected heavy ion-like signals
 discovered in small systems by LHC experiments [11, 12, 35].

5. Conclusion

282 Motivated by the results of our previous work [26], where we shown that the
 particle production sensitive to the underlying event (UE observables) exhibited
 an approximate KNO scaling. In this paper we investigated in more detail the
 285 scaling properties using data from three experiments at the LHC, as well as
 their description using multiple partonic interactions and color reconnection in
 the context of PYTHIA 8 (version 8.212 tune Monash 2013) event generator.

288 We studied the number density in the transverse side divided by the charged-

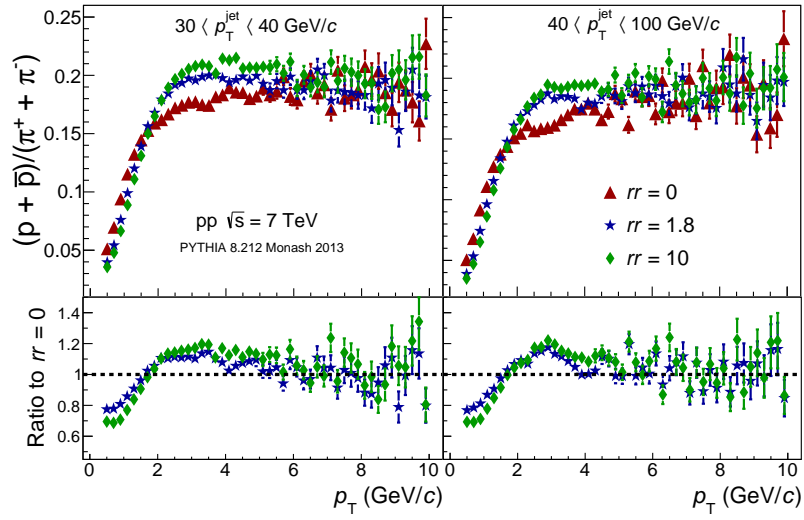


Figure 5: (Color online). Proton-to-pion ratio in the UE as a function of the hadron transverse momentum for different values of reconnection range in two p_T^{jet} intervals: 30-40 GeV/c (left) and 40-100 GeV/c (right). Bottom panels show the variation of the proton-to-pion ratio with respect to $rr = 0$. Error bars indicate the statistical uncertainties.

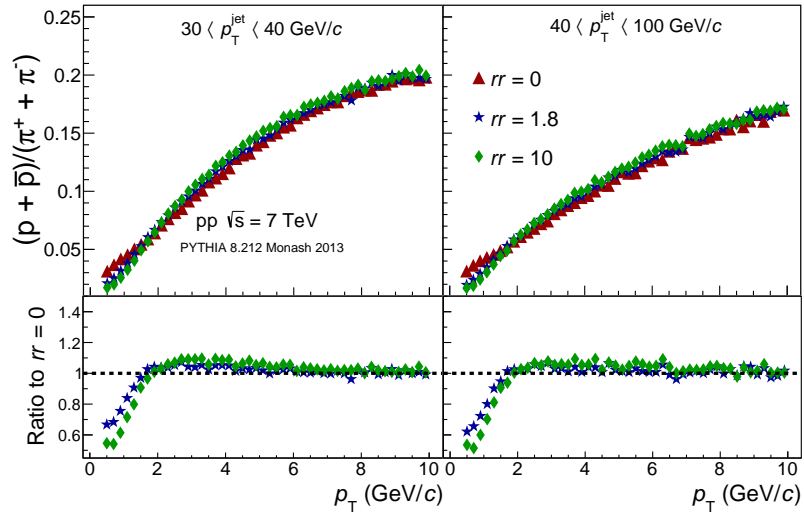


Figure 6: (Color online). Proton-to-pion ratio in the jet region and within $R < 0.5$ as a function of the hadron transverse momentum for different values of reconnection range in two p_T^{jet} intervals: 30-40 GeV/c (left) and 40-100 GeV/c (right). Bottom panels show the variation of the proton-to-pion ratio with respect to $rr = 0$. Error bars indicate the statistical uncertainties.

particle density in inelastic pp collisions (KNO variable). Both two quantities were calculated considering charged-particles with $p_T > 0.5 \text{ GeV}/c$. The ratio was found to increase with increasing \sqrt{s} , the trend was well described by PYTHIA 8. In particular going from pp collisions at $\sqrt{s} = 0.9$ to 7 TeV, the ratio increased by 8-10%. In PYTHIA 8 the rate of such an increase with increasing \sqrt{s} was close to that for multiple partonic interactions. Moreover, using the limited available data we found indications that particle production at intermediate- p_T ($2 < p_T < 10 \text{ GeV}/c$) increased faster in UE than in inelastic events. Whereas at lower p_T , such an increase in both UE and inelastic events was the same within uncertainties. This effect could yield the small breaking (10%) of the KNO scaling in the particle production sensitive to UE.

The results above motivated the study of the traditional underlying-event observables considering particles within different p_T intervals. We found that color reconnection modifies the p_T spectra of unidentified charged particles, producing a variation in the number and summed- p_T densities. In short, color reconnection enhanced the particle production at intermediate transverse momenta in regions far from the jet peaks. The modification was mass dependent, e.g. the proton-to-pion ratio as a function of p_T in the underlying-event region exhibited a flow-like response with the variation of the color reconnection strength. This behavior was very similar to what was observed in the bulk (everything outside the jet peak) region measured in heavy-ion collisions.

Our paper encourages the measurement of p_T spectra of unidentified and identified charged particles in the transverse side. The variation of such p_T spectra as a function of center-of-mass energy, p_T^{jet} (or p_T^{leading}), and system size would add key information on the origin of the heavy ion-like effects observed in pp collisions.

6. Acknowledgments

We acknowledge the technical support of Luciano Diaz and Eduardo Murrieta for the maintenance and operation of the computing farm at ICN-UNAM.

318 Support for this work has been received from CONACyT under the Grant No.
280362 and PAPIIT-UNAM under Project No. IN102118.

References

- 321 [1] T. Sjöstrand, M. van Zijl, A multiple-interaction model for the event
structure in hadron collisions, *Phys. Rev. D* 36 (1987) 2019–2041. doi:
10.1103/PhysRevD.36.2019.
- 324 [2] B. Abelev, et al., Transverse sphericity of primary charged particles in
minimum bias proton-proton collisions at $\sqrt{s} = 0.9, 2.76$ and 7 TeV,
Eur. Phys. J. C 72 (2012) 2124. arXiv:1205.3963, doi:10.1140/epjc/
327 s10052-012-2124-9.
- [3] T. Martin, P. Skands, S. Farrington, Probing Collective Effects in Hadro-
nisation with the Extremes of the Underlying Event, *Eur. Phys. J. C* 76 (5)
330 (2016) 299. arXiv:1603.05298, doi:10.1140/epjc/s10052-016-4135-4.
- [4] R. Harnik, T. Wizansky, Signals of New Physics in the Underlying
Event, *Phys. Rev. D* 80 (2009) 075015. arXiv:0810.3948, doi:10.1103/
333 PhysRevD.80.075015.
- [5] D. Acosta, et al., The underlying event in hard interactions at the Tevatron
 $\bar{p}p$ collider, *Phys. Rev. D* 70 (2004) 072002. arXiv:hep-ex/0404004, doi:
336 10.1103/PhysRevD.70.072002.
- [6] T. Aaltonen, et al., Studying the Underlying Event in Drell-Yan and High
Transverse Momentum Jet Production at the Tevatron, *Phys. Rev. D* 82
339 (2010) 034001. arXiv:1003.3146, doi:10.1103/PhysRevD.82.034001.
- [7] G. Aad, et al., Measurement of underlying event characteristics using
charged particles in pp collisions at $\sqrt{s} = 900\text{GeV}$ and 7 TeV with
342 the ATLAS detector, *Phys. Rev. D* 83 (2011) 112001. arXiv:1012.0791,
doi:10.1103/PhysRevD.83.112001.

- [8] M. Aaboud, et al., Measurement of charged-particle distributions sensitive
345 to the underlying event in $\sqrt{s} = 13$ TeV proton-proton collisions with the
ATLAS detector at the LHC, JHEP 03 (2017) 157. [arXiv:1701.05390](#),
[doi:10.1007/JHEP03\(2017\)157](#).
- [9] A. Ortiz, Mean p_T scaling with m/n_q at the LHC: Absence of (hydro)
348 flow in small systems?, Nucl. Phys. A943 (2015) 9–17. [arXiv:1506.00584](#),
[doi:10.1016/j.nuclphysa.2015.08.003](#).
- [10] B. B. Abelev, et al., Multiplicity Dependence of Pion, Kaon, Proton and
351 Lambda Production in p-Pb Collisions at $\sqrt{s_{NN}} = 5.02$ TeV, Phys. Lett.
B728 (2014) 25–38. [arXiv:1307.6796](#), [doi:10.1016/j.physletb.2013.](#)
354 [11.020](#).
- [11] V. Khachatryan, et al., Evidence for collectivity in pp collisions at the LHC,
Phys. Lett. B765 (2017) 193–220. [arXiv:1606.06198](#), [doi:10.1016/j.](#)
357 [physletb.2016.12.009](#).
- [12] J. Adam, et al., Enhanced production of multi-strange hadrons in high-
multiplicity proton-proton collisions, Nature Phys. 13 (2017) 535–539.
360 [arXiv:1606.07424](#), [doi:10.1038/nphys4111](#).
- [13] T. Sjöstrand, S. Ask, J. R. Christiansen, R. Corke, N. Desai, P. Ilten,
S. Mrenna, S. Prestel, C. O. Rasmussen, P. Z. Skands, An Introduction
363 to PYTHIA 8.2, Comput. Phys. Commun. 191 (2015) 159–177. [arXiv:](#)
[1410.3012](#), [doi:10.1016/j.cpc.2015.01.024](#).
- [14] A. Ortiz Velasquez, P. Christiansen, E. Cuautle Flores, I. Maldonado Cer-
366 vantes, G. Paić, Color Reconnection and Flowlike Patterns in pp Colli-
sions, Phys. Rev. Lett. 111 (4) (2013) 042001. [arXiv:1303.6326](#), [doi:](#)
[10.1103/PhysRevLett.111.042001](#).
- [15] B. Abelev, et al., Multiplicity dependence of two-particle azimuthal correla-
369 tions in pp collisions at the LHC, JHEP 09 (2013) 049. [arXiv:1307.1249](#),
[doi:10.1007/JHEP09\(2013\)049](#).

- 372 [16] A. Ortiz, G. Bencedi, H. Bello, Revealing the source of the radial flow patterns in proton–proton collisions using hard probes, *J. Phys. G* 44 (6) (2017) 065001. [arXiv:1608.04784](#), [doi:10.1088/1361-6471/aa6594](#).
- 375 [17] S. G. Weber, A. Dubla, A. Andronic, A. Morsch, Multiplicity dependent J/ψ production in proton-proton collisions with PYTHIA8 [arXiv:1811.07744](#).
- 378 [18] M. Veldhoen, p/π Ratio in Di-Hadron Correlations, *Nucl. Phys. A* 910-911 (2013) 306–309. [arXiv:1207.7195](#), [doi:10.1016/j.nuclphysa.2012.12.103](#).
- 381 [19] T. O. H. Richert, Λ/K_s^0 associated with a jet in central Pb-Pb collisions at $\sqrt{s_{NN}} = 2.76$ TeV measured with the ALICE detector, Ph.D. thesis, Lund U. (2016-05-16).
- 384 [20] P. Skands, S. Carrazza, J. Rojo, Tuning PYTHIA 8.1: the Monash 2013 Tune, *Eur. Phys. J. C* 74 (8) (2014) 3024. [arXiv:1404.5630](#), [doi:10.1140/epjc/s10052-014-3024-y](#).
- 387 [21] S. Chatrchyan, et al., Measurement of the Underlying Event Activity at the LHC with $\sqrt{s} = 7$ TeV and Comparison with $\sqrt{s} = 0.9$ TeV, *JHEP* 09 (2011) 109. [arXiv:1107.0330](#), [doi:10.1007/JHEP09\(2011\)109](#).
- 390 [22] B. Abelev, et al., Underlying Event measurements in pp collisions at $\sqrt{s} = 0.9$ and 7 TeV with the ALICE experiment at the LHC, *JHEP* 07 (2012) 116. [arXiv:1112.2082](#), [doi:10.1007/JHEP07\(2012\)116](#).
- 393 [23] E. Maguire, L. Heinrich, G. Watt, HEPData: a repository for high energy physics data, *J. Phys. Conf. Ser.* 898 (10) (2017) 102006. [arXiv:1704.05473](#), [doi:10.1088/1742-6596/898/10/102006](#).
- 396 [24] G. P. Salam, G. Soyez, A Practical Seedless Infrared-Safe Cone jet algorithm, *JHEP* 05 (2007) 086. [arXiv:0704.0292](#), [doi:10.1088/1126-6708/2007/05/086](#).

- 399 [25] M. Cacciari, G. P. Salam, G. Soyez, FastJet User Manual, Eur. Phys. J. C72
(2012) 1896. [arXiv:1111.6097](#), [doi:10.1140/epjc/s10052-012-1896-2](#).
- [26] A. Ortiz, L. Valencia Palomo, Universality of the underlying event in pp
402 collisions, Phys. Rev. D96 (11) (2017) 114019. [arXiv:1710.04741](#), [doi:10.1103/PhysRevD.96.114019](#).
- [27] V. Khachatryan, et al., Transverse momentum and pseudorapidity distri-
405 butions of charged hadrons in pp collisions at $\sqrt{s} = 0.9$ and 2.36 TeV,
JHEP 02 (2010) 041. [arXiv:1002.0621](#), [doi:10.1007/JHEP02\(2010\)041](#).
- [28] V. Khachatryan, et al., Transverse-momentum and pseudorapidity distri-
408 butions of charged hadrons in *pp* collisions at $\sqrt{s} = 7$ TeV, Phys. Rev.
Lett. 105 (2010) 022002. [arXiv:1005.3299](#), [doi:10.1103/PhysRevLett.105.022002](#).
- 411 [29] B. B. Abelev, et al., Energy Dependence of the Transverse Momentum
Distributions of Charged Particles in pp Collisions Measured by ALICE,
Eur. Phys. J. C73 (12) (2013) 2662. [arXiv:1307.1093](#), [doi:10.1140/epjc/s10052-013-2662-9](#).
414
- [30] V. Khachatryan, et al., Measurement of the underlying event activity us-
ing charged-particle jets in proton-proton collisions at $\sqrt{s} = 2.76$ TeV,
417 JHEP 09 (2015) 137. [arXiv:1507.07229](#), [doi:10.1007/JHEP09\(2015\)137](#).
- [31] Z. Koba, H. B. Nielsen, P. Olesen, Scaling of multiplicity distributions
420 in high-energy hadron collisions, Nucl. Phys. B40 (1972) 317–334. [doi:10.1016/0550-3213\(72\)90551-2](#).
- [32] T. Sjöstrand, Collective Effects: the viewpoint of HEP MC codes, 2018.
423 [arXiv:1808.03117](#).
- [33] A. Ortiz, Experimental results on event shapes at hadron colliders, Adv.
Ser. Direct. High Energy Phys. 29 (2018) 343–357. [arXiv:1705.02056](#),
426 [doi:10.1142/9789813227767_0016](#).

- [34] J. Adam, et al., Centrality dependence of the nuclear modification factor of charged pions, kaons, and protons in Pb-Pb collisions at $\sqrt{s_{\text{NN}}} = 2.76$ TeV, Phys. Rev. C93 (3) (2016) 034913. [arXiv:1506.07287](#), [doi:10.1103/PhysRevC.93.034913](#).
429
- [35] S. Acharya, et al., Multiplicity dependence of light-flavor hadron production in pp collisions at $\sqrt{s} = 7$ TeV, Submitted to: Phys. Rev. [CarXiv:1807.11321](#).
432